JOURNAL OF MAGNETIC RESONANCE 77, 258–273 (1988)

# A Product Operator Description of AB and ABX Spin Systems

LEWIS E. KAY

*Department of Molecular Biophysics and Biochemistry, Yale University, New Haven, Connecticut 06511*

AND

R. E. D. MCCLUNG

*Department of Chemistry, University of Alberta, Edmonton, Alberta, Canada T6G 2G2*

Received June 20, 1987

A simple product operator description of the strongly coupled AB and ABX spin systems is developed. The utility of this description in the investigation of the effects of strong coupling is illustrated in a number of examples. © 1988 Academic Press, Inc.

## INTRODUCTION

The product operator representation of the density operator devised by Sørensen *et al.* (*1*) and by Packer and Wright (*2*) has revolutionized the way in which the evolution of weakly coupled spin systems in modern NMR experiments is described. The product operator description is so much more compact and comprehensive than the detailed element-by-element density matrix description that even the most complex 2D NMR experiments can be described with ease. Motivated by the success of the product operator descriptions of weakly coupled spin systems (*1, 2*), we have investigated product operator descriptions for the AB and ABX strongly coupled spin systems. Kumar *et al.* (*3, 4*) have investigated the behavior of these spin systems during various spin-echo and multiple-quantum coherence experiments using element-by-element density matrix calculations, and have shown the analysis to be very complicated.

In this paper, we investigate the behavior of the simple product basis operators (developed for weakly coupled spin systems) under the influence of Zeeman and strong scalar coupling. Some simple examples are present to demonstrate the utility of the product operator description in strongly coupled systems.

## THEORY

*AB spin system.* For a strongly coupled two-spin system, the spin Hamiltonian $\mathscr{H}$ (in $s^{-1}$) in the absence of RF fields is

$$\mathscr{H} = \omega_A A_z + \omega_B B_z + 2\pi J_{AB}(A_z B_z + A_x B_x + A_y B_y), \quad [1]$$

where $A_m$ and $B_m$ are the $m$ components of the spin angular momentum operators for nuclei A and B, $\omega_A$ and $\omega_B$ are the precession frequencies (in $s^{-1}$) of A and B, and $J_{AB}$ is the scalar-coupling constant (in Hz). It is useful to write $\mathscr{H}$ in the form



0022-2364/88 $3.00
Copyright © 1988 by Academic Press, Inc.
All rights of reproduction in any form reserved.

$$\mathscr{H} = \mathscr{H}_0 + \mathscr{H}_1, \quad [2]$$

where

$$\mathscr{H}_0 = \bar{\omega}(A_z + B_z) + 2\pi J_{AB}(A_z B_z), \quad [3]$$

and

$$\mathscr{H}_1 = \delta\omega(A_z - B_z) + 2\pi J_{AB}(A_x B_x + A_y B_y), \quad [4]$$

where $\bar{\omega} = (\omega_A + \omega_B)/2$ and $\delta\omega = (\omega_A - \omega_B)/2$. This separation of the Hamiltonian is useful since

$$[\mathscr{H}_0, \mathscr{H}_1] = 0 \quad [5]$$

allows one to express the evolution of the density operator, $\rho$, during a period of free precession as

$$\begin{aligned}\rho(t) &= \exp(-i\mathscr{H}t)\rho(0)\exp(i\mathscr{H}t) \\ &= \exp(-i\mathscr{H}_0 t)\{\exp(-i\mathscr{H}_1 t)\rho(0)\exp(i\mathscr{H}_1 t)\}\exp(i\mathscr{H}_0 t), \quad [6]\end{aligned}$$

and to consider the evolutions under $\mathscr{H}_0$ and under $\mathscr{H}_1$ separately. The evolution of the spin product operators belonging to coherence levels $\pm 1$ in the spherical basis (*5*) under $\mathscr{H}_0$ and under $\mathscr{H}_1$ is given in Table 1.

The results in Table 1 were derived by the procedure outlined by Slichter (*6*). As an illustration, we show how the operator $A_{+1}$ evolves under $\mathscr{H}_1$. Consider the operator, $f(t)$, defined by

$$f(t) = \exp(-i\mathscr{H}_1 t)A_{+1}\exp(i\mathscr{H}_1 t). \quad [7]$$

TABLE 1

Transformation of Coherence Level ±1 Operators for AB Spin System

$$A_{\pm 1} \xrightarrow{\mathscr{H}_1 t} A_{\pm 1}a_1(\pm t) + 2A_0B_{\pm 1}a_2(\pm t)$$

$$2A_{\pm 1}B_0 \xrightarrow{\mathscr{H}_1 t} 2A_{\pm 1}B_0a_1(\pm t) + B_{\pm 1}a_2(\pm t)$$

$$B_{\pm 1} \xrightarrow{\mathscr{H}_1 t} B_{\pm 1}a_1(\mp t) + 2A_{\pm 1}B_0a_2(\pm t)$$

$$2A_0B_{\pm 1} \xrightarrow{\mathscr{H}_1 t} 2A_0B_{\pm 1}a_1(\mp t) + A_{\pm 1}a_2(\pm t)$$

$$A_{\pm 1} \xrightarrow{\mathscr{H}_0 t} A_{\pm 1}b_1(\pm t) + 2A_{\pm 1}B_0b_2(\pm t)$$

$$2A_{\pm 1}B_0 \xrightarrow{\mathscr{H}_0 t} 2A_{\pm 1}B_0b_1(\pm t) + A_{\pm 1}b_2(\pm t)$$

$$B_{\pm 1} \xrightarrow{\mathscr{H}_0 t} B_{\pm 1}b_1(\pm t) + 2A_0B_{\pm 1}b_2(\pm t)$$

$$2A_0B_{\pm 1} \xrightarrow{\mathscr{H}_0 t} 2A_0B_{\pm 1}b_1(\pm t) + B_{\pm 1}b_2(\pm t)$$

$$a_1(t) = \cos(\Lambda t) - i(\delta\omega/\Lambda)\sin(\Lambda t), \quad a_2(t) = i(\pi J_{AB}/\Lambda)\sin(\Lambda t)$$

$$b_1(t) = \cos(\pi J_{AB}t)\exp(-i\bar{\omega}t), \quad b_2(t) = -i\sin(\pi J_{AB}t)\exp(-i\bar{\omega}t)$$

$$\Lambda = \sqrt{(\delta\omega)^2 + (\pi J_{AB})^2}$$

The time derivative of $f(t)$ is

$$\frac{df}{dt} = i\exp(-i\mathscr{H}_1 t)[A_{+1}, \mathscr{H}_1]\exp(i\mathscr{H}_1 t)$$

$$= i\exp(-i\mathscr{H}_1 t)\{-\delta\omega A_{+1} + \pi J_{AB}(2A_0 B_{+1})\}\exp(i\mathscr{H}_1 t), \quad [8]$$

and the second derivative is

$$\frac{d^2 f}{dt^2} = -\{(\delta\omega)^2 + (\pi J_{AB})^2\} f = -\Lambda^2 f. \quad [9]$$

The solution to differential equation [9] shows that $A_{+1}$ transforms under $\mathscr{H}_1$ according to

$$A_{+1} \xrightarrow{\mathscr{H}_1 t} A_{+1} a_1(t) + 2A_0 B_{+1} a_2(t), \quad [10]$$

where $a_1(t)$ and $a_2(t)$ are defined in Table 1. The formulas for the evolution of the other coherence level ±1 product operators were derived in an analogous fashion. The frequency $\Lambda$ defined in Table 1 is the usual frequency variable which arises in the analysis of the AB spectrum (*7*). The results in Table 1 are valid only for spin-$\frac{1}{2}$ nuclei since the evaluation of commutators like $[2A_0 B_{+1}, A_x B_x + A_y B_y]$ yields trilinear forms like $A_{+1}A_0 B_0$ which can be reduced to simple basis operators only when both A and B have spin-$\frac{1}{2}$.

When one considers the effect of $\mathscr{H}_1$ on the operators $A_0$ and $B_0$, one obtains a set of four coupled differential equations involving the operators $A_0$, $B_0$, $A_{+1}B_{-1}$, and $A_{-1}B_{+1}$. Simplification is obtained by forming the differential equations for linear combinations of these operators, and one ultimately obtains the results in Table 2. The operators $A_0$, $B_0$, $2A_{+1}B_{-1}$, and $2A_{-1}B_{+1}$ commute with $\mathscr{H}_0$, so the effects of free precession on these operators are completely described by their evolution under $\mathscr{H}_1$. It is interesting to note that the longitudinal magnetizations $A_0$ and $B_0$ oscillate at

TABLE 2

Transformation of Coherence Level 0 Operators for AB Spin System

$$A_0 \xrightarrow{\mathscr{H}_1 t} A_0 r_1(t) + B_0 r_2(t) + 2A_{+1}B_{-1} r_3(t) + 2A_{-1}B_{+1} r_3(-t)$$

$$B_0 \xrightarrow{\mathscr{H}_1 t} A_0 r_2(t) + B_0 r_1(t) - 2A_{+1}B_{-1} r_3(t) - 2A_{-1}B_{+1} r_3(-t)$$

$$2A_{+1}B_{-1} \xrightarrow{\mathscr{H}_1 t} A_0 r_3(t) - B_0 r_3(t) + 2A_{+1}B_{-1} r_4(t) + 2A_{-1}B_{+1} r_2(t)$$

$$2A_{-1}B_{+1} \xrightarrow{\mathscr{H}_1 t} A_0 r_3(-t) - B_0 r_3(-t) + 2A_{+1}B_{-1} r_2(t) + 2A_{-1}B_{+1} r_4(-t)$$

$$r_1(t) = \{1 + [(\delta\omega)^2 + (\pi J_{AB})^2\cos(2\Lambda t)]/\Lambda^2\}/2$$

$$r_2(t) = (\pi J_{AB}/\Lambda)^2\{1 - \cos(2\Lambda t)\}/2$$

$$r_3(t) = (\pi J_{AB}/\Lambda)\{(\delta\omega/\Lambda)[\cos(2\Lambda t) - 1] - i\sin(2\Lambda t)\}/2$$

$$r_4(t) = \{\cos(2\Lambda t) + [(\pi J_{AB})^2 + (\delta\omega)^2\cos(2\Lambda t)]/\Lambda^2 - 2i(\delta\omega/\Lambda)\sin(2\Lambda t)\}/2$$

frequency $2\Lambda$ (Table 2), while the transverse magnetizations oscillate at frequency $\Lambda$ under $\mathscr{H}_1$.

Braunschweiler and Ernst (*8*) have considered the evolution of the Cartesian basis product operators for the AB spin system under the spin–spin coupling interaction $2\pi J_{AB}\mathbf{A}\cdot\mathbf{B}$. The results in Tables 1 and 2 reduce to their results for the case $\delta\omega = \bar{\omega} = 0$.

*ABX spin system.* For the three-spin ABX system, the free precession Hamiltonian can be written as

$$\mathscr{H} = \omega_A A_z + \omega_B B_z + \omega_X X_z + 2\pi J_{AB}(A_z B_z + A_x B_x + A_y B_y) + 2\pi J_{AX} A_z X_z + 2\pi J_{BX} B_z X_z, \quad [11]$$

where $A_m$, $B_m$, and $X_m$ are the $m$- components of the nuclear spin angular momentum operators; $\omega_A$, $\omega_B$, and $\omega_X$ are the precession frequencies of the nuclei A, B, and X respectively. In Eq. [11], spins A and B are strongly coupled with coupling constant $J_{AB}$ (Hz), and spins A and B are weakly coupled to spin X with respective coupling constants $J_{AX}$ and $J_{BX}$. In a fashion which is exactly analogous to the AB case, we separate the spin Hamiltonian in Eq. [11] into

$$\mathscr{H}_0 = \bar{\omega}(A_z + B_z) + \omega_X X_z + 2\pi\bar{J}(A_z + B_z)X_z + 2\pi J_{AB} A_z B_z, \quad [12]$$

and

$$\mathscr{H}_1 = \delta\omega(A_z - B_z) + 2\pi\delta J(A_z - B_z)X_z + 2\pi J_{AB}(A_x B_x + A_y B_y), \quad [13]$$

where $\bar{\omega} = (\omega_A + \omega_B)/2$, $\bar{J} = (J_{AX} + J_{BX})/2$, and $\delta J = (J_{AX} - J_{BX})/2$. We again obtain the simplification in Eq. [6] because $\mathscr{H}_0$ and $\mathscr{H}_1$ commute. As in the AB case, the evolution of the product operators under $\mathscr{H}_0$ and under $\mathscr{H}_1$ can be derived by the method of Slichter (*6*), and the results for spin operators belonging to coherence levels $+1$ and $-1$ are given in Table 2.

It should be noted that appropriate linear combinations of product operators are used in the analysis in order to obtain uncoupled differential equations. As an example we derive the result for the evolution of $A_{+1}$ under $\mathscr{H}_1$. Consider the operators $g_\pm(t)$ defined by

$$g_\pm(t) = \exp(-i\mathscr{H}_1 t)\{A_{+1} \pm 2A_{+1}X_0\}\exp(i\mathscr{H}_1 t), \quad [14]$$

with first derivative

$$\frac{dg_\pm(t)}{dt} = i\exp(-i\mathscr{H}_1 t)[A_{+1} \pm 2A_{+1}X_0, \mathscr{H}_1]\exp(i\mathscr{H}_1 t)$$

$$= i\exp(-i\mathscr{H}_1 t)\{-(\delta\omega \pm \pi\delta J)(A_{+1}X_0) + \pi J_{AB}(2A_0 B_{+1} \pm 4A_0 B_{+1}X_0)\}\exp(i\mathscr{H}_1 t) \quad [15]$$

and second derivative

$$\frac{d^2 g_\pm(t)}{dt^2} = -[(\delta\omega \pm \pi\delta J)^2 + (\pi J_{AB})^2]g_\pm(t) = -\Lambda_\pm^2 g_\pm(t). \quad [16]$$

The solutions to Eq. [16] for $g_+(t)$ and $g_-(t)$ are easily manipulated to show that the transformation of $A_{+1}$ under $\mathscr{H}_1$ is given by

$$A_{+1} \xrightarrow{\mathscr{H}_1} A_{+1}f_1(t) + 2A_{+1}X_0f_2(t) + 2A_0B_{+1}f_3(t) + 4A_0B_{+1}X_0f_4(t), \quad [17]$$

where the functions $f_i(t)$ are defined in Table 3. The formulas for the evolution of the other coherence level $\pm 1$ product operators are derived in an analogous fashion. The frequency variables $\Lambda_+$ and $\Lambda_-$ defined in Table 3 are the standard frequencies which arise in the analysis of the ABX spectrum (*7*).

The evolution of $X_{\pm 1}$ under $\mathscr{H}_1$ is much more difficult to derive since one encounters two sets of six coupled differential equations involving operators $X_{\pm 1}$, $2A_0X_{\pm 1}$, $2B_0X_{\pm 1}$, $4A_0B_0X_{\pm 1}$, $4A_{-1}B_{+1}X_{\pm 1}$, and $4A_{+1}B_{-1}X_{\pm 1}$. The evolution of the operators belonging to coherence level $-1$ is given in Table 4. The evolution of operators belonging to coherence level $+1$ can be derived from the results in Table 4 using the property

$$I_\mu^* = (-1)^\mu I_{-\mu}, \quad [18]$$

where $I_\mu$ is the $\mu$th spherical component of spin angular momentum for nucleus I.

The description of the evolution of operators for the ABX spin system which belong to coherence level 0 involves a set of eight coupled differential equations in the operators $A_0$, $B_0$, $2A_{+1}B_{-1}$, $2A_{-1}B_{+1}$, $2A_0X_0$, $2B_0X_0$, $4A_{+1}B_{-1}X_0$, and $4A_{-1}B_{+1}X_0$. The solution of this set of equations gives the evolution of each of these operators under $\mathscr{H}_1$, as shown in Table 5. $X_0$ commutes with both $\mathscr{H}_0$ and $\mathscr{H}_1$, so it is unchanged during free precession. Similarly, the other operators belonging to coherence level 0 commute with $\mathscr{H}_0$, so one need be concerned only with the effects of $\mathscr{H}_1$ on these operators during a period of free precession.

It should be noted that the effect of $\mathscr{H}_1$ in both AB and ABX systems is to generate periodic transfer of magnetization between the strongly coupled nuclei A and B (*4*). For example, the *A*-magnetization component $A_{+1}$ is transferred to antiphase *B*-magnetization component $2A_0B_{+1}$ under $\mathscr{H}_1$ (see Tables 1 and 3). The *z* magnetizations $A_0$ and $B_0$ of the AB spin system undergo periodic exchange and are involved in transfer with the zero-quantum "combination" modes $2A_{+1}B_{-1}$ and $2A_{-1}B_{+1}$. Similar exchanges between the *z* magnetizations of the AB part of ABX, and transfers to combination modes, occur in the ABX spin system. Surprisingly, the behavior of the coherence level $-1$ operators for the X part of ABX (Table 4) is more complicated than the behavior of the corresponding operators for the AB part of ABX (Table 3) since transfer between transverse *X* magnetization and combination modes $4A_{+1}B_{-1}X_{-1}$ and $4A_{-1}B_{+1}X_{-1}$ occurs. As expected, the results in Tables 1–5 indicate that free precession allows interchange between operators in the same coherence level. Changes in coherence level occur only when RF fields are applied (*5, 9, 10*).

## APPLICATIONS

In this section, we illustrate the utility of the product operator description of strongly coupled systems discussed above by considering several one- and two-dimensional NMR experiments. In particular, we consider the AB and ABX spin systems, and focus our attention on the features in the experiments which can be attributed to the effects of strong coupling. The applications discussed below have been investigated using a version of the computer simulation system described earlier (*1*) which has been modified to handle the evolution of the $\pm 1$ coherence level operators of the AB

TABLE 3

Transformation of Coherence Level ±1 Operators for AB Part of ABX Spin System

$$A_{\pm1} \xrightarrow{\mathscr{H}_1 t} A_{\pm1}f_1(\pm t) + 2A_{\pm1}X_0 f_2(\pm t) + 2A_0B_{\pm1}f_3(\pm t) + 4A_0B_{\pm1}X_0 f_4(\pm t)$$

$$B_{\pm1} \xrightarrow{\mathscr{H}_1 t} B_{\pm1}f_1(\mp t) + 2B_{\pm1}X_0 f_2(\mp t) + 2A_{\pm1}B_0 f_3(\pm t) + 4A_{\pm1}B_0X_0 f_4(\pm t)$$

$$2A_{\pm1}X_0 \xrightarrow{\mathscr{H}_1 t} 2A_{\pm1}X_0 f_1(\pm t) + A_{\pm1}f_2(\pm t) + 4A_0B_{\pm1}X_0 f_3(\pm t) + 2A_0B_{\pm1}f_4(\pm t)$$

$$2B_{\pm1}X_0 \xrightarrow{\mathscr{H}_1 t} 2B_{\pm1}X_0 f_1(\mp t) + B_{\pm1}f_2(\mp t) + 4A_{\pm1}B_0X_0 f_3(\pm t) + 2A_{\pm1}B_0 f_4(\pm t)$$

$$2A_{\pm1}B_0 \xrightarrow{\mathscr{H}_1 t} 2A_{\pm1}B_0 f_1(\pm t) + 4A_{\pm1}B_0X_0 f_2(\pm t) + B_{\pm1}f_3(\pm t) + 2B_{\pm1}X_0 f_4(\pm t)$$

$$2A_0B_{\pm1} \xrightarrow{\mathscr{H}_1 t} 2A_0B_{\pm1}f_1(\mp t) + 4A_0B_{\pm1}X_0 f_2(\mp t) + A_{\pm1}f_3(\pm t) + 2A_{\pm1}X_0 f_4(\pm t)$$

$$4A_{\pm1}B_0X_0 \xrightarrow{\mathscr{H}_1 t} 4A_{\pm1}B_0X_0 f_1(\pm t) + 2A_{\pm1}B_0 f_2(\pm t) + 2B_{\pm1}X_0 f_3(\pm t) + B_{\pm1}f_4(\pm t)$$

$$4A_0B_{\pm1}X_0 \xrightarrow{\mathscr{H}_1 t} 4A_0B_{\pm1}X_0 f_1(\mp t) + 2A_0B_{\pm1}f_2(\mp t) + 2A_{\pm1}X_0 f_3(\pm t) + A_{\pm1}f_4(\pm t)$$

$$A_{\pm1} \xrightarrow{\mathscr{H}_0 t} A_{\pm1}g_1(\pm t) + 2A_{\pm1}B_0 g_2(\pm t) + 2A_{\pm1}X_0 g_3(\pm t) + 4A_{\pm1}B_0X_0 g_4(\pm t)$$

$$B_{\pm1} \xrightarrow{\mathscr{H}_0 t} B_{\pm1}g_1(\pm t) + 2A_0B_{\pm1}g_2(\pm t) + 2B_{\pm1}X_0 g_3(\pm t) + 4A_0B_{\pm1}X_0 g_4(\pm t)$$

$$2A_{\pm1}X_0 \xrightarrow{\mathscr{H}_0 t} 2A_{\pm1}X_0 g_1(\pm t) + 4A_{\pm1}B_0X_0 g_2(\pm t) + A_{\pm1}g_3(\pm t) + 2A_{\pm1}B_0 g_4(\pm t)$$

$$2B_{\pm1}X_0 \xrightarrow{\mathscr{H}_0 t} 2B_{\pm1}X_0 g_1(\pm t) + 4A_0B_{\pm1}X_0 g_2(\pm t) + B_{\pm1}g_3(\pm t) + 2A_0B_{\pm1}g_4(\pm t)$$

$$2A_{\pm1}B_0 \xrightarrow{\mathscr{H}_0 t} 2A_{\pm1}B_0 g_1(\pm t) + A_{\pm1}g_2(\pm t) + 4A_{\pm1}B_0X_0 g_3(\pm t) + 2A_{\pm1}X_0 g_4(\pm t)$$

$$2A_0B_{\pm1} \xrightarrow{\mathscr{H}_0 t} 2A_0B_{\pm1}g_1(\pm t) + B_{\pm1}g_2(\pm t) + 4A_0B_{\pm1}X_0 g_3(\pm t) + 2B_{\pm1}X_0 g_4(\pm t)$$

$$4A_{\pm1}B_0X_0 \xrightarrow{\mathscr{H}_0 t} 4A_{\pm1}B_0X_0 g_1(\pm t) + 2A_{\pm1}X_0 g_2(\pm t) + 2A_{\pm1}B_0 g_3(\pm t) + A_{\pm1}g_4(\pm t)$$

$$4A_0B_{\pm1}X_0 \xrightarrow{\mathscr{H}_0 t} 4A_0B_{\pm1}X_0 g_1(\pm t) + 2B_{\pm1}X_0 g_2(\pm t) + 2A_0B_{\pm1}g_3(\pm t) + B_{\pm1}g_4(\pm t)$$

$$f_1(t) = \{c_-\exp(i\Lambda_+ t) + c_+\exp(-i\Lambda_+ t) + d_-\exp(i\Lambda_- t) + d_+\exp(-i\Lambda_- t)\}/4$$

$$f_2(t) = \{c_-\exp(i\Lambda_+ t) + c_+\exp(-i\Lambda_+ t) - d_-\exp(i\Lambda_- t) - d_+\exp(-i\Lambda_- t)\}/4$$

$$f_3(t) = (i/2)\{(\pi J_{AB}/\Lambda_+)\sin(\Lambda_+ t) + (\pi J_{AB}/\Lambda_-)\sin(\Lambda_- t)\}$$

$$f_4(t) = (i/2)\{(\pi J_{AB}/\Lambda_+)\sin(\Lambda_+ t) - (\pi J_{AB}/\Lambda_-)\sin(\Lambda_- t)\}$$

$$\Lambda_\pm = \sqrt{(\delta\omega \pm \pi\delta J)^2 + (\pi J_{AB})^2}, \quad c_\pm = 1 \pm (\delta\omega + \pi\delta J)/\Lambda_+, \quad d_\pm = 1 \pm (\delta\omega - \pi\delta J)/\Lambda_-$$

$$g_1(t) = (1/2)\{\cos[\pi(\bar{J} + J_{AB})t] + \cos[\pi(\bar{J} - J_{AB})t]\}\exp(-i\bar{\omega}t)$$

$$g_2(t) = (-i/2)\{\sin[\pi(\bar{J} + J_{AB})t] - \sin[\pi(\bar{J} - J_{AB})t]\}\exp(-i\bar{\omega}t)$$

$$g_3(t) = (-i/2)\{\sin[\pi(\bar{J} + J_{AB})t] + \sin[\pi(\bar{J} - J_{AB})t]\}\exp(-i\bar{\omega}t)$$

$$g_4(t) = (1/2)\{\cos[\pi(\bar{J} + J_{AB})t] - \cos[\pi(\bar{J} - J_{AB})t]\}\exp(-i\bar{\omega}t)$$

TABLE 4
Transformation of Coherence Level −1 Operators for X Part of ABX Spin System

$$X_{-1} \xrightarrow{\mathscr{H}_1 t} X_{-1}s_1(t) + 4A_0B_0X_{-1}s_2(t) + 2A_0X_{-1}s_3(t) - 2B_0X_{-1}s_3(t) - 4A_{+1}B_{-1}X_{-1}s_4(t) + 4A_{-1}B_{+1}X_{-1}s_4(-t)$$

$$4A_0B_0X_{-1} \xrightarrow{\mathscr{H}_1 t} X_{-1}s_2(t) + 4A_0B_0X_{-1}s_1(t) - 2A_0X_{-1}s_3(t) + 2B_0X_{-1}s_3(t) + 4A_{+1}B_{-1}X_{-1}s_4(t) - 4A_{-1}B_{+1}X_{-1}s_4(-t)$$

$$2A_0X_{-1} \xrightarrow{\mathscr{H}_1 t} X_{-1}s_3(t) - 4A_0B_0X_{-1}s_3(t) + 2A_0X_{-1}s_5(t) + 2B_0X_{-1}s_6(t) + 4A_{+1}B_{-1}X_{-1}s_7(t) + 4A_{-1}B_{+1}X_{-1}s_7(-t)$$

$$2B_0X_{-1} \xrightarrow{\mathscr{H}_1 t} -X_{-1}s_3(t) + 4A_0B_0X_{-1}s_3(t) + 2A_0X_{-1}s_6(t) + 2B_0X_{-1}s_5(t) - 4A_{+1}B_{-1}X_{-1}s_7(t) - 4A_{-1}B_{+1}X_{-1}s_7(-t)$$

$$4A_{+1}B_{-1}X_{-1} \xrightarrow{\mathscr{H}_1 t} -X_{-1}s_4(t) + 4A_0B_0X_{-1}s_4(t) + 2A_0X_{-1}s_7(t) - 2B_0X_{-1}s_7(t) + 4A_{+1}B_{-1}X_{-1}s_8(t) + 4A_{-1}B_{+1}X_{-1}s_9(t)$$

$$4A_{-1}B_{+1}X_{-1} \xrightarrow{\mathscr{H}_1 t} X_{-1}s_4(-t) - 4A_0B_0X_{-1}s_4(-t) + 2A_0X_{-1}s_7(-t) - 2B_0X_{-1}s_7(-t) + 4A_{+1}B_{-1}X_{-1}s_9(t) + 4A_{-1}B_{+1}X_{-1}s_8(-t)$$

$$s_1(t) = 1/2 + (A/2)[u_-\cos(\Omega_+t) - u_+\cos(\Omega_-t)]$$

$$s_2(t) = 1/2 - (A/2)[u_-\cos(\Omega_+t) - u_+\cos(\Omega_-t)]$$

$$s_3(t) = [iA/(4\pi\delta J)][\Omega_+u_-\sin(\Omega_+t) - \Omega_-u_+\sin(\Omega_-t)]$$

$$s_4(t) = [u_+u_-A/(8\pi^2J_{AB}\delta J)][\cos(\Omega_+t) - \cos(\Omega_-t) - i(2\delta\omega/\Omega_+)\sin(\Omega_+t) + i(2\delta\omega/\Omega_-)\sin(\Omega_-t)]$$

$$s_5(t) = 1/2 - (A/2)[v_+\cos(\Omega_+t) - v_-\cos(\Omega_-t)]$$

$$s_6(t) = 1/2 + (A/2)[v_+\cos(\Omega_+t) - v_-\cos(\Omega_-t)]$$

$$s_7(t) = -\pi J_{AB}A\{2\delta\omega[\cos(\Omega_+t) - \cos(\Omega_-t)] - i\Omega_+\sin(\Omega_+t) + i\Omega_-\sin(\Omega_-t)\}$$

$$s_8(t) = -A\{[u_+ - 2(\pi J_{AB})^2]\cos(\Omega_+t) - [u_- - 2(\pi J_{AB})^2]\cos(\Omega_-t) + i[2\delta\omega/(\Omega_+\Omega_-)][\Omega_-u_+\sin(\Omega_+t) - \Omega_+u_-\sin(\Omega_-t)]\}$$

$$s_9(t) = 2A(\pi J_{AB})^2[\cos(\Omega_+t) - \cos(\Omega_-t)]$$

$$\Omega_\pm = \Lambda_+ \pm \Lambda_-, \quad A = 1/(\Omega_-^2 - \Omega_+^2), \quad u_\pm = \Omega_\pm^2 - (2\pi\delta J)^2, \quad v_\pm = \Omega_\pm^2 - (2\delta\omega)^2$$

$$X_{\pm1} \xrightarrow{\mathscr{H}_0 t} X_{\pm1}j_1(\pm t) + 2A_0X_{\pm1}j_2(\pm t) + 2B_0X_{\pm1}j_2(\pm t) + 4A_0B_0X_{\pm1}j_3(\pm t)$$

$$2A_0X_{\pm1} \xrightarrow{\mathscr{H}_0 t} X_{\pm1}j_2(\pm t) + 2A_0X_{\pm1}j_1(\pm t) + 2B_0X_{\pm1}j_3(\pm t) + 4A_0B_0X_{\pm1}j_2(\pm t)$$

$$2B_0X_{\pm1} \xrightarrow{\mathscr{H}_0 t} X_{\pm1}j_2(\pm t) + 2A_0X_{\pm1}j_3(\pm t) + 2B_0X_{\pm1}j_1(\pm t) + 4A_0B_0X_{\pm1}j_2(\pm t)$$

$$4A_0B_0X_{\pm1} \xrightarrow{\mathscr{H}_0 t} X_{\pm1}j_3(\pm t) + 2A_0X_{\pm1}j_2(\pm t) + 2B_0X_{\pm1}j_2(\pm t) + 4A_0B_0X_{\pm1}j_1(\pm t)$$

$$j_1(t) = (1/2)[1 + \cos(2\pi\bar{J}t)]\exp(-i\omega_X t)$$

$$j_2(t) = (-i/2)\sin(2\pi\bar{J}t)\exp(-i\omega_X t)$$

$$j_3(t) = (1/2)[-1 + \cos(2\pi\bar{J}t)]\exp(-i\omega_X t)$$

TABLE 5

Transformation of Coherence Level 0 Operators for AB Part of ABX Spin System

$$A_0 \xrightarrow{\mathscr{H}_1 t} A_0 q_1(t) + B_0 q_2(t) + 2A_{+1}B_{-1}q_3(t) + 2A_{-1}B_{+1}q_3(-t) - 2A_0X_0q_4(t) + 2B_0X_0q_4(t) + 4A_{+1}B_{-1}X_0q_5(t) + 4A_{-1}B_{+1}X_0q_5(-t)$$

$$B_0 \xrightarrow{\mathscr{H}_1 t} A_0 q_2(t) + B_0 q_1(t) - 2A_{+1}B_{-1}q_3(t) - 2A_{-1}B_{+1}q_3(-t) + 2A_0X_0q_4(t) - 2B_0X_0q_4(t) - 4A_{+1}B_{-1}X_0q_5(t) - 4A_{-1}B_{+1}X_0q_5(-t)$$

$$2A_{+1}B_{-1} \xrightarrow{\mathscr{H}_1 t} A_0 q_3(t) - B_0 q_3(t) + 2A_{+1}B_{-1}q_6(t) + 2A_{-1}B_{+1}q_2(t) + 2A_0X_0q_5(t) - 2B_0X_0q_5(t) + 4A_{+1}B_{-1}X_0q_7(t) + 4A_{-1}B_{+1}X_0q_4(t)$$

$$2A_{-1}B_{+1} \xrightarrow{\mathscr{H}_1 t} A_0 q_3(-t) - B_0 q_3(-t) + 2A_{+1}B_{-1}q_2(t) + 2A_{-1}B_{+1}q_6(-t) + 2A_0X_0q_5(-t) - 2B_0X_0q_5(-t) + 4A_{+1}B_{-1}X_0q_4(t) + 4A_{-1}B_{+1}X_0q_7(-t)$$

$$2A_0X_0 \xrightarrow{\mathscr{H}_1 t} -A_0 q_4(t) + B_0 q_4(t) + 2A_{+1}B_{-1}q_5(t) + 2A_{-1}B_{+1}q_5(-t) + 2A_0X_0q_1(t) + 2B_0X_0q_2(t) + 4A_{+1}B_{-1}X_0q_3(t) + 4A_{-1}B_{+1}X_0q_3(-t)$$

$$2B_0X_0 \xrightarrow{\mathscr{H}_1 t} A_0 q_4(t) - B_0 q_4(t) - 2A_{+1}B_{-1}q_5(t) - 2A_{-1}B_{+1}q_5(-t) + 2A_0X_0q_2(t) + 2B_0X_0q_1(t) - 4A_{+1}B_{-1}X_0q_3(t) - 4A_{-1}B_{+1}X_0q_3(-t)$$

$$4A_{+1}B_{-1}X_0 \xrightarrow{\mathscr{H}_1 t} A_0 q_5(t) - B_0 q_5(t) + 2A_{+1}B_{-1}q_7(t) + 2A_{-1}B_{+1}q_4(t) + 2A_0X_0q_3(t) - 2B_0X_0q_3(t) + 4A_{+1}B_{-1}X_0q_6(t) + 4A_{-1}B_{+1}X_0q_2(t)$$

$$4A_{-1}B_{+1}X_0 \xrightarrow{\mathscr{H}_1 t} A_0 q_5(-t) - B_0 q_5(-t) + 2A_{+1}B_{-1}q_4(t) + 2A_{-1}B_{+1}q_7(-t) + 2A_0X_0q_3(-t) - 2B_0X_0q_3(-t) + 4A_{+1}B_{-1}X_0q_2(t) + 4A_{-1}B_{+1}X_0q_6(-t)$$

$$q_1(t) = (1/4)\{2 + [(\delta\omega + \pi\delta J)^2 + (\pi J_{AB})^2\cos(2\Lambda_+ t)]/\Lambda_+^2 + [(\delta\omega - \pi\delta J)^2 + (\pi J_{AB})^2\cos(2\Lambda_- t)]/\Lambda_-^2\}$$

$$q_2(t) = [\pi J_{AB}/(2\Lambda_+)]^2[1 - \cos(2\Lambda_+ t)] + [\pi J_{AB}/(2\Lambda_-)]^2[1 - \cos(2\Lambda_- t)]$$

$$q_3(t) = [(\pi J_{AB})/(4\Lambda_+)]\{[(\delta\omega + \pi\delta J)/\Lambda_+][\cos(2\Lambda_+ t) - 1] - i\sin(2\Lambda_+ t)\} + [(\pi J_{AB})/(4\Lambda_-)]\{[(\delta\omega - \pi\delta J)/\Lambda_-][\cos(2\Lambda_- t) - 1] - i\sin(2\Lambda_- t)\}$$

$$q_4(t) = [\pi J_{AB}/(2\Lambda_+)]^2[\cos(2\Lambda_+ t) - 1] - [\pi J_{AB}/(2\Lambda_-)]^2[\cos(2\Lambda_- t) - 1]$$

$$q_5(t) = [(\pi J_{AB})/(4\Lambda_+)]\{[(\delta\omega + \pi\delta J)/\Lambda_+][1 - \cos(2\Lambda_+ t)] + i\sin(2\Lambda_+ t)\} - [(\pi J_{AB})/(4\Lambda_-)]\{[(\delta\omega - \pi\delta J)/\Lambda_-][1 - \cos(2\Lambda_- t)] - i\sin(2\Lambda_- t)\}$$

$$q_6(t) = (1/4)\{2\cos(2\Lambda_+ t) - 2i[(\delta\omega + \pi\delta J)/\Lambda_+]\sin(2\Lambda_+ t) - (\pi J_{AB}/\Lambda_+)^2[\cos(2\Lambda_+ t) - 1]\} + (1/4)\{2\cos(2\Lambda_- t) - 2i[(\delta\omega - \pi\delta J)/\Lambda_-]\sin(2\Lambda_- t) - (\pi J_{AB}/\Lambda_-)^2[\cos(2\Lambda_- t) - 1]\}$$

$$q_7(t) = -(1/4)\{2\cos(2\Lambda_+ t) - 2i[(\delta\omega + \pi\delta J)/\Lambda_+]\sin(2\Lambda_+ t) - (\pi J_{AB}/\Lambda_+)^2[\cos(2\Lambda_+ t) - 1]\} + (1/4)\{2\cos(2\Lambda_- t) - 2i[(\delta\omega - \pi\delta J)/\Lambda_-]\sin(2\Lambda_- t) - (\pi J_{AB}/\Lambda_-)^2[\cos(2\Lambda_- t) - 1]\}$$

spin system (Table 1), and the AB part of the ABX spin system (Table 3). In all examples, we have assumed perfect quadrature detection so that observed signals are associated with operators $A_{-1}$, $B_{-1}$, and $X_{-1}$ only.

*(a) $\pi/2$-Acquire.* We consider the sequence $(\pi/2)_x$-$t$ applied to an AB spin system at thermal equilibrium. The evolution of the density operator follows the scheme

$$A_0 + B_0 \xrightarrow{(\pi/2)(A_x + B_x)} -(i/\sqrt{2})(A_{-1} + B_{-1} + A_{+1} + B_{+1})$$

$$-(i/\sqrt{2})(A_{-1} + B_{-1}) \xrightarrow{\mathscr{H}t} (-i/\sqrt{2})\{A_{-1}[a_1(-t)b_1(-t) + a_2(-t)b_2(-t)] + B_{-1}[a_1(t)b_1(-t) + a_2(-t)b_2(-t)]\}. \quad [19]$$

The $A_{+1} + B_{+1}$ terms produced by the pulse have been ignored since they do not produce observable signals. The terms involving $2A_{-1}B_0$ and $2A_0B_{-1}$ which develop from $A_{-1}$ and $B_{-1}$ during the evolution under $\mathscr{H}_0$ and $\mathscr{H}_1$ have been omitted from the final result in Eq. [18] because the observed signal is obtained from the sum of the coefficients of $A_{-1}$ and $B_{-1}$ only. The acquired signal is proportional to

$$S(t) = (1 - \pi J_{AB}/\Lambda)\{\exp[i(\bar{\omega} + \Lambda + \pi J_{AB})t] + \exp[i(\bar{\omega} - \Lambda - \pi J_{AB})t]\} + (1 + \pi J_{AB}/\Lambda)\{\exp[i(\bar{\omega} + \Lambda - \pi J_{AB})t] + \exp[i(\bar{\omega} - \Lambda + \pi J_{AB})t]\} \quad [20]$$

and the corresponding frequency spectrum consists of lines at frequencies $\bar{\omega} \pm (\Lambda + \pi J_{AB})$ with intensity $1 - \pi J_{AB}/\Lambda$, and at frequencies $\bar{\omega} \pm (\Lambda - \pi J_{AB})$ with intensity $1 + \pi J_{AB}/\Lambda$. This is, of course, the "classic" AB spectrum (7) and has been derived here without any reference to eigenfunctions of the spin Hamiltonian.

For the ABX system, the evolution of the density operator through the $(\pi/2)_x$-$t$ pulse sequence is given by

$$A_0 + B_0 + X_0 \xrightarrow{(\pi/2)(A_x + B_x + X_x)} (-i/\sqrt{2})(A_{-1} + B_{-1} + X_{-1} + A_{+1} + B_{+1} + X_{+1})$$

$$(-i/\sqrt{2})(A_{-1} + B_{-1} + X_{-1}) \xrightarrow{\mathscr{H}t} (i/\sqrt{2})A_{-1}\{f_1(-t)g_1(-t) + f_2(-t)g_3(-t) + f_3(-t)g_2(-t) + f_4(-t)g_4(-t)\} + (-i/\sqrt{2})B_{-1}\{f_1(t)g_1(-t) + f_2(t)g_3(-t) + f_3(-t)g_4(-t) + f_4(-t)g_2(-t)\} + (-i/\sqrt{2})X_{-1}\{s_1(t)j_1(-t) + s_2(t)j_3(-t)\}. \quad [21]$$

The acquired signal here is just the sum of the coefficients of $A_{-1}$, $B_{-1}$, and $X_{-1}$ in the density operator and is proportional to

$$\begin{aligned} S(t) = {} & (1 - \pi J_{AB}/\Lambda_+) \\ & \times \{\exp[i(\bar{\omega} + \pi\bar{J} + \Lambda_+ + \pi J_{AB})t] + \exp[i(\bar{\omega} + \pi\bar{J} - \Lambda_+ - \pi J_{AB})t]\} \\ & + (1 + \pi J_{AB}/\Lambda_+)\{\exp[i(\bar{\omega} + \pi\bar{J} + \Lambda_+ - \pi J_{AB})t] + \exp[i(\bar{\omega} + \pi\bar{J} - \Lambda_+ + \pi J_{AB})t]\} \\ & + (1 + \pi J_{AB}/\Lambda_-)\{\exp[i(\bar{\omega} - \pi\bar{J} + \Lambda_- - \pi J_{AB})t] + \exp[i(\bar{\omega} - \pi\bar{J} - \Lambda_- + \pi J_{AB})t]\} \\ & + (1 - \pi J_{AB}/\Lambda_-)\{\exp[i(\bar{\omega} - \pi\bar{J} + \Lambda_- + \pi J_{AB})t] + \exp[(\bar{\omega} - \pi\bar{J} - \Lambda_- - \pi J_{AB})t]\} \end{aligned}$$

$$+ (1/2)\{1 - [(\delta\omega)^2 - (\pi\delta J)^2 + (\pi J_{AB})^2]/\Lambda_+\Lambda_-)\}\{\exp[i(\omega_X + \Lambda_+ + \Lambda_-)t]$$
$$+ \exp[i(\omega_X - \Lambda_+ - \Lambda_-)t]\} + (1/2)\{1 + [(\delta\omega)^2 - (\pi\delta J)^2 + (\pi J_{AB})^2]/\Lambda_+\Lambda_-)\}$$
$$\times \{\exp[i(\omega_X + \Lambda_+ - \Lambda_-)t] + \exp[i(\omega_X - \Lambda_+ + \Lambda_-)t]\}$$
$$+ \{\exp[i(\omega_X + \pi\bar{J})t] + \exp[i(\omega_X - \pi\bar{J})t]\}. \quad [22]$$

The corresponding frequency spectrum consists of lines at frequencies $\bar{\omega} + \pi\bar{J} \pm (\Lambda_+ + \pi J_{AB})$ with intensity $1 - \pi J_{AB}/\Lambda_+$, at frequencies $\bar{\omega} + \pi\bar{J} \pm (\Lambda_+ - \pi J_{AB})$ with intensity $1 + \pi J_{AB}/\Lambda_+$, at frequencies $\bar{\omega} - \pi\bar{J} \pm (\Lambda_- - \pi J_{AB})$ with intensity $1 + \pi J_{AB}/\Lambda_-$, at frequencies $\bar{\omega} - \pi\bar{J} \pm (\Lambda_- + \pi J_{AB})$ with intensity $1 - \pi J_{AB}/\Lambda_-$, at frequencies $\omega_X \pm (\Lambda_+ + \Lambda_-)$ with intensity $\{1 - [(\delta\omega)^2 - (\pi\delta J)^2 + (\pi J_{AB})^2]/(\Lambda_+\Lambda_-)\}/2$, and at frequencies $\omega_X \pm (\Lambda_+ - \Lambda_-)$ and $\omega_X \pm \pi\bar{J}$ with intensities $\{1 + [(\delta\omega)^2 - (\pi\delta J)^2 + (\pi J_{AB})^2]/(\Lambda_+\Lambda_-)\}/2$ and 1, respectively. These frequencies and intensities agree with those given by Pople, Schneider, and Bernstein (*7*).

*(b) 2D Homonuclear J-resolved experiment.* When the pulse sequence $(\pi/2)_x$–$(t_1/2)$–$(\pi)_x$–$(t_1/2 + t_2)$ is applied to an AB spin system, the density operator follows the scheme

$$A_0 + B_0 \xrightarrow{(\pi/2)(A_x + B_x)} \xrightarrow{\mathcal{H}t_1/2} \xrightarrow{\pi(A_x + B_x)} \xrightarrow{\mathcal{H}t_1/2}$$
$$(i\sqrt{2})\{(A_{-1} + B_{-1})\cos(\pi J_{AB}t_1) + i(2A_{-1}B_0 + 2A_0B_{-1})\sin(\pi J_{AB}t_1)\}$$
$$\times \{(\delta\omega/\Lambda)^2 + (\pi J_{AB}/\Lambda)^2\cos(\Lambda t_1)\}$$
$$+ (i/\sqrt{2})\{(A_{-1} + B_{-1})\sin(\pi J_{AB}t_1) - i(2A_{-1}B_0 + 2A_0B_{-1})\cos(\pi J_{AB}t_1)\}$$
$$\times \{(\pi J_{AB}/\Lambda)\sin(\Lambda t_1)\}$$
$$+ (1/\sqrt{2})\{(A_{-1} - B_{-1})\sin(\pi J_{AB}t_1) + i(2A_{-1}B_0 - 2A_0B_{-1})\cos(\pi J_{AB}t_1)\}$$
$$\times \{(\delta\omega/\Lambda)(\pi J_{AB}/\Lambda)[\cos(\Lambda t_1) - 1]\}$$
$$\xrightarrow{\mathcal{H}t_2} (i/\sqrt{2})(A_{-1} + B_{-1})\{(\delta\omega/\Lambda)^2\cos(\pi J_{AB}t_1 + \pi J_{AB}t_2)\cos(\Lambda t_2)$$
$$+ (\pi J_{AB}/\Lambda)\sin(\pi J_{AB}t_1 + \pi J_{AB}t_2)\sin(\Lambda t_1 + \Lambda t_2)$$
$$+ (\pi J_{AB}/\Lambda)^2\cos(\pi J_{AB}t_1 + \pi J_{AB}t_2)\cos(\Lambda t_1 + \Lambda t_2)\}\exp(i\bar{\omega}t_2). \quad [23]$$

The terms containing $(\pi J_{AB}/\Lambda)$ in the density operator at time $t_1$ and at time $t_1 + t_2$ result from strong coupling of A and B. Detailed investigation of the evolution of the density operator shows that the $A_0$ term in $\rho(0)$ generates terms in $\rho(t_1/2)$ which contain $A_{+1}$, $2A_{+1}B_0$, $B_{+1}$, and $2A_0B_{+1}$. Each of these terms produce identical contributions to each of the strong coupling terms in $\rho(t_1)$, and hence in $\rho(t_1 + t_2)$. One cannot, therefore, attribute the strong coupling terms in $\rho(t_1 + t_2)$ to one or two particular terms which arise at intermediate points in the sequence because strong coupling effects occur in all precession periods.

The acquired signal in the 2D *J*-resolved experiment on the AB spin system (see Eq. [23]) gives "normal" peaks at frequencies $[\omega_1, \omega_2] = [\pi J_{AB}, \bar{\omega} \pm \Lambda + \pi J_{AB}]$ and $[-\pi J_{AB}, \bar{\omega} \pm \Lambda - \pi J_{AB}]$ with intensity $(\delta\omega/\Lambda)^2$, and "unexpected" peaks, due to strong coupling, at frequencies $[\pm(\Lambda + \pi J_{AB}), \bar{\omega} \pm (\Lambda + \pi J_{AB})]$ with intensity $(\pi J_{AB}/\Lambda)(-1$

$+ \pi J_{AB}/\Lambda)$ and at frequencies $[\pm(\Lambda - \pi J_{AB}), \bar{\omega} \pm (\Lambda - \pi J_{AB})]$ with intensity $(\pi J_{AB}/\Lambda)(1 + \pi J_{AB}/\Lambda)$. The features in the *J*-resolved experiment due to strong coupling agree with the results of Kumar (*3*), and with experimental observations (*11, 12*).

The ABX homonuclear spin system gives rise to similar results in the 2D *J*-resolved pulse sequence and one obtains the frequencies and intensities given by Kumar (*3*).

*(c) NOESY with zero mixing time.* The appearance of additional peaks in 2D NMR spectra due to strong coupling is not limited to *J*-resolved experiments. Recently a study of the effects of strong coupling on NOESY spectra indicated that cross peaks between spins A and B could arise purely from scalar coupling (*13*). In order to elucidate these features, we consider the behavior of AB and ABX spin systems during the pulse sequence $(\pi/2)_x$–$t_1$–$(\pi/2)_x$–$\tau$–$(\pi/2)_x$–$t_2$. We assume that the mixing time $\tau$ is short compared to all relaxation times so that no cross-relaxation occurs in this interval; hence $\tau$ is set to zero and all relaxation is ignored. For the AB spin system, the density operator during the "zero mixing time" NOESY experiment follows the scheme

$$A_0 + B_0 \xrightarrow{(\pi/2)(A_x + B_x)} \xrightarrow{\mathscr{H} t_1} \xrightarrow{(\pi/2)(A_x + B_x)}$$

$$\{-(1/2)(A_0 + B_0)[\cos(\Lambda t_1)\cos(\pi J_{AB} t_1) + (\pi J_{AB}/\Lambda)\sin(\Lambda t_1)\sin(\pi J_{AB} t_1)]$$

$$- (i/2)(A_0 - B_0)[(\delta\omega/\Lambda)\sin(\Lambda t_1)\cos(\pi J_{AB} t_1)]\}\exp(i\bar{\omega} t_1)$$

$$\xrightarrow{(\pi/2)(A_x + B_x)} \xrightarrow{\mathscr{H} t_2}$$

$$(A_{-1} + B_{-1})\{(i\sqrt{2}/4)[\cos(\Lambda t_1 + \Lambda t_2)\cos(\pi J_{AB} t_1)\cos(\pi J_{AB} t_2)]$$

$$+ i(\sqrt{2}/4)(\pi J_{AB}/\Lambda)^2[\sin(\Lambda t_1)\sin(\Lambda t_2)\cos(\pi J_{AB} t_1 - \pi J_{AB} t_2)]$$

$$+ (i\sqrt{2}/8)(\pi J_{AB}/\Lambda)[\sin(\Lambda t_1 + \Lambda t_2)\sin(\pi J_{AB} t_1 + \pi J_{AB} t_2)$$

$$+ \sin(\Lambda t_1 - \Lambda t_2)\sin(\pi J_{AB} t_1 - \pi J_{AB} t_2)]\}\exp[i(\bar{\omega} t_1 + \bar{\omega} t_2)], \quad [24]$$

where the terms in $\rho(t_1^+)$ containing $(\pi J_{AB}/\Lambda)$ and the terms in $\rho(t_1 + t_2)$ containing $(\pi J_{AB}/\Lambda)$ and $(\pi J_{AB}/\Lambda)^2$ arise because of strong coupling between nuclei A and B. In Eq. [24], we have considered only the $-1$ coherence level terms during the $t_1$ and $t_2$ periods ("*P*-type" peaks), and only the $z$ magnetizations in the mixing period. This latter restriction avoids the complications from zero-quantum combination modes, which give rise to the so-called "*J* peaks" in NOESY 2D maps (*14*). Experimentally, this suppression of zero-quantum coherences is achieved by the application of a gradient pulse at the start of the mixing period, or by stochastic variation of the length of the mixing time (*14*).

The terms in $\rho(t_1 + t_2)$ (see Eq. [24]) show that, in addition to the expected "diagonal" peaks at frequencies $[\omega_1, \omega_2] = [\bar{\omega} \pm (\Lambda + \pi J_{AB}), \bar{\omega} \pm (\Lambda + \pi J_{AB})]$, $[\bar{\omega} \pm (\Lambda - \pi J_{AB}), \bar{\omega} \pm (\Lambda - \pi J_{AB})]$, $[(\bar{\omega} \pm (\Lambda + \pi J_{AB}), \bar{\omega} \pm (\Lambda - \pi J_{AB})]$, and $[\bar{\omega} \pm (\Lambda - \pi J_{AB}), \bar{\omega} \pm (\Lambda + \pi J_{AB})]$ which have relative intensities $(1 - \pi J_{AB}/\Lambda)$, $(1 + \pi J_{AB}/\Lambda)$, $(\delta\omega/\Lambda)^2$, and $(\delta\omega/\Lambda)^2$, respectively, A–B cross peaks with frequencies $[\bar{\omega} \pm (\Lambda + \pi J_{AB}), \bar{\omega} \mp (\Lambda + \pi J_{AB})]$, and $[\bar{\omega} \pm (\Lambda - \pi J_{AB}), \bar{\omega} \mp (\Lambda - \pi J_{AB})]$ with relative intensities $(\pi J_{AB}/\Lambda)(-1 + (\pi J_{AB}/\Lambda)$ and $(\pi J_{AB}/\Lambda)(1 + \pi J_{AB}/\Lambda)$, respectively, appear in the 2D map. These cross peaks are due entirely to the presence of strong coupling between nuclei A and B, and will also occur in the usual NOESY experiment with nonzero mixing time.

The cross peaks which one might expect at frequencies $[\bar{\omega} \pm (\Lambda + \pi J_{AB}), \bar{\omega} \mp (\Lambda - \pi J_{AB})]$ and $[\bar{\omega} \pm (\Lambda - \pi J_{AB}), \bar{\omega} \mp (\Lambda + \pi J_{AB})]$ have zero intensity.

The results of a "zero mixing time" NOESY experiment on 2,6-dicarboxynaphthalene, an AB spin system, displayed in absolute value mode, and the corresponding density matrix simulated 2D map (*13*) are shown in Fig. 1. The appearance of A–B cross peaks with frequencies $[\bar{\omega} \pm (\Lambda + \pi J_{AB}), \bar{\omega} \mp (\Lambda + \pi J_{AB})]$ and $[\bar{\omega} \pm (\Lambda - \pi J_{AB}), \bar{\omega} \mp (\Lambda - \pi J_{AB})]$ with opposite phases, but no cross peaks at frequencies $[\bar{\omega} \pm (\Lambda + \pi J_{AB}), \bar{\omega} \mp (\Lambda - \pi J_{AB})]$ and $[\bar{\omega} \pm (\Lambda - \pi J_{AB}), \bar{\omega} \mp (\Lambda + \pi J_{AB})]$, agree with the predictions of the product operator calculation given above. Several features of the 2D maps shown in Fig. 1 warrant comment. First, cross peaks between A and B spins are observed, despite the fact that the mixing period is much too short for any cross-relaxation to occur, and that stochastic variation of the mixing time restricts the signal to those components which are derived from $z$ magnetization during the mixing period. Second, the multiplet components of the cross peaks in the simulated spectrum vary in both phase and intensity, in contrast to cross peaks derived from cross-relaxation which would have the same phase and similar intensities (*14*). It is proposed, therefore, that in NOESY data sets with sufficiently high resolution, one may distinguish between cross peaks arising from strong coupling effects and cross peaks arising from cross-relaxation by the relative phases of the multiplet components and their relative intensities.

The behavior of the AB part of the ABX spin system during the zero mixing time NOESY experiment is exactly analogous to the behavior of the AB spin system. One finds A–B cross peaks at frequencies $[\bar{\omega} \pm (\Lambda_+ + \pi J_{AB}) + \pi \bar{J}, \bar{\omega} \mp (\Lambda_+ + \pi J_{AB}) + \pi \bar{J}]$, $[\bar{\omega} \pm (\Lambda_+ - \pi J_{AB}) + \pi \bar{J}, \omega \mp (\Lambda_+ - \pi J_{AB}) + \bar{J}]$, $[\bar{\omega} \pm (\Lambda_- + J_{AB}) - \pi \bar{J}, \bar{\omega} \mp (\Lambda_- + \pi J_{AB}) - \pi \bar{J}]$, and $[\bar{\omega} \pm (\Lambda_- - \pi J_{AB}) - \pi \bar{J}, \bar{\omega} \mp (\Lambda_- - \pi J_{AB}) - \pi \bar{J}]$ with intensities proportional to $(\pi J_{AB}/\Lambda_+)(-1 + \pi J_{AB}/\Lambda_+)$, $(\pi J_{AB}/\Lambda_+)(1 + \pi J_{AB}/\Lambda_+)$, $(\pi J_{AB}/\Lambda_-)(-1 + \pi J_{AB}/\Lambda_-)$, and $(\pi J_{AB}/\Lambda_-)(1 + \pi J_{AB}/\Lambda_-)$, respectively. No cross peaks are predicted between the AB and X parts of the spectrum. The X part of the 2D map has diagonal peaks at $\omega_1 = \omega_2 = \bar{\omega}_X \pm \bar{J}/2$, $\omega_X \pm (\Lambda_+ - \Lambda_-)$ and off-diagonal peaks between all of the multiplet lines. The strong coupling between A and B nuclei produces only small effects on the

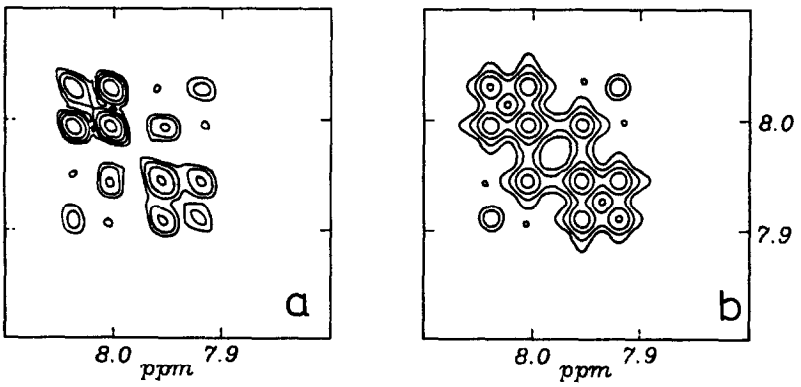


FIG. 1. Contour plots of AB region of experimental (a) and simulated (b) NOESY experiment with zero mixing time on 2,6-dicarboxynaphthalene [see Ref. (*13*) for simulation parameters].

intensities of some of the peaks, and these effects arise from the exchange of $X_{-1}$ magnetization with the combination modes $4A_{\pm 1}B_{\mp 1}X_{-1}$ during $t_1$.

The $(\pi/2)_x$–$\tau$–$(\pi/2)_x$ part of the zero mixing time NOESY experiment is a $z$ filter (*15*) which has been applied in other sequences. The effects of the $z$ filter on strongly coupled spin systems described above can be expected in these other experiments too.

*(d) "Unexpected" peaks in C–H correlation experiments.* In proton-decoupled 2D DEPT experiments (*5, 16*) and in conventional 2D DEPT experiments (*16, 17*), one finds unexpected C–H correlation peaks between protons bonded to one carbon atom with the adjacent carbon atom(s) in addition to the expected "directly bonded" correlations. These unexpected correlation peaks are found to have significant intensity when the difference in vicinal proton chemical shifts is approximately equal to the directly bonded $^1H$–$^{13}C$ coupling constant, and are believed to arise from strong coupling effects. Although these features are observed in a number of correlation experiments, we shall concentrate on the simplest preparation–evolution sequence $(\pi/2)_x^H$–$t_1/2$–$(\pi)_x^C$–$t_1/2$, and study the behavior of the fragment

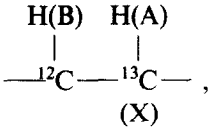


an ABX spin system, during this sequence. The pulses which are appended to this preparation–evolution sequence, in order to obtain heteronuclear correlation, convert transverse $A$ magnetization to transverse $X$ magnetization. We are therefore interested in the terms in the density operator containing operator $A_{-1}$ at the end of the evolution period, since the final detected $X_{-1}$ magnetization is derived from these terms.

It is useful to recognize that the propagator

$$\xrightarrow{(\pi/2)(A_x + B_x)} \xrightarrow{(\mathscr{H}_0 + \mathscr{H}_1)t_1/2} \xrightarrow{\pi X_x} \xrightarrow{(\mathscr{H}_0 + \mathscr{H}_1)t_1/2}$$

is equivalent to the propagator

$$\xrightarrow{(\pi/2)(A_x + B_x)} \xrightarrow{\mathscr{H}_1 t_1/2} \xrightarrow{\pi X_x} \xrightarrow{\mathscr{H}_1 t_1/2} \xrightarrow{[\bar{\omega}(A_z + B_z) + 2\pi J_{AB}A_zB_z]t_1}$$

[see Ref. (*1*)] since this allows separate investigation of the effects of $\mathscr{H}_1$ and $\mathscr{H}_0$. The evolution of the density operator through this preparation–evolution sequence is

$$A_0 + B_0 \xrightarrow{(\pi/2)(A_x + B_x)} \xrightarrow{\mathscr{H}_1 t_1/2} \xrightarrow{\pi X_x} \xrightarrow{\mathscr{H}_1 t_1/2}$$

$$A_{-1}L_A(t_1) + 2A_{-1}B_0L_B(t_1) \xrightarrow{[\bar{\omega}(A_z + B_z) + 2\pi J_{AB}A_zB_z]t_1}$$

$$A_{-1}\{L_A(t_1)\cos(\pi J_{AB}t_1)e^{i\bar{\omega}t_1} + iL_B(t_1)\sin(\pi J_{AB}t_1)e^{i\bar{\omega}t_1}\}, \quad [25]$$

where

$$L_A \propto [c_+d_+ + (\pi J_{AB})^2/(\Lambda_+\Lambda_-)]\exp[i(\Lambda_+ + \Lambda_-)t_1/2]$$
$$+ [c_+d_- - (\pi J_{AB})^2/(\Lambda_+\Lambda_-)]\exp[i(\Lambda_+ - \Lambda_-)t_1/2]$$

$$+ [c_- d_+ - (\pi J_{AB})^2/(\Lambda_+\Lambda_-)]\exp[-i(\Lambda_+ - \Lambda_-)t_1/2]$$

$$+ [c_- d_- + (\pi J_{AB})^2/(\Lambda_+\Lambda_-)]\exp[-i(\Lambda_+ + \Lambda_-)t_1/2], \quad [26]$$

and

$$L_B \propto \pi J_{AB}(1/\Lambda_+ + 1/\Lambda_-)\{\exp[i(\Lambda_+ + \Lambda_-)t_1/2] - \exp[-i(\Lambda_+ + \Lambda_-)t_1/2]\}$$

$$+ \pi J_{AB}(1/\Lambda_+ - 1/\Lambda_-)\{\exp[i(\Lambda_+ - \Lambda_-)t_1/2] - \exp[-i(\Lambda_+ - \Lambda_-)t_1/2]\}. \quad [27]$$

In Eq. [25], only the $A_{-1}$ terms are given in the final density operator, since only these terms are converted to $X_{-1}$ magnetization and reach the detector in the final stages of the heteronuclear correlation experiment. The term containing $L_A(t_1)$ originates from the $A_0$ term in the initial density operator, while the $L_B(t_1)$ term originates from $B_0$. The oscillation frequencies of the various terms in $L_A(t_1)$ and $L_B(t_1)$ are conveniently classified as

$$\Lambda_+ + \Lambda_- = \bar{\omega}_A \qquad \text{"average A,"}$$

$$-(\Lambda_+ + \Lambda_-) = \bar{\omega}_B \qquad \text{"average B,"}$$

and

$$\Lambda_+ - \Lambda_- = \bar{\omega}_{AB} \qquad \text{"average A + B"}$$

since they correspond to averages of resonance frequencies in the AB part of the ABX spectrum. In the weak coupling limit where $\delta\omega \gg \delta J$, $L_A(t_1)$ is dominated by the term with frequency $\bar{\omega}_A$, and $L_B(t_1)$ by small terms with frequencies $\bar{\omega}_A$ and $\bar{\omega}_B$. As $\delta\omega$ decreases compared to $\delta J$, the magnitudes of the terms in $L_B(t_1)$ with frequencies $\bar{\omega}_A$ and $\bar{\omega}_B$ increase, and $L_A(t_1)$ continues to be dominated by the $\bar{\omega}_A$ term. Terms in both $L_A(t_1)$ and $L_B(t_1)$ with average A + B frequencies also grow in magnitude. It is clear that the term in $L_B(t_1)$ with frequency $\bar{\omega}_B$ gives rise to the "unexpected" B–X correlation peak in the 2D heteronuclear correlation map since, after the magnetization transfer part of the sequence, it will produce a term proportional to

$$X_{-1}\exp(i\omega_x t_2)\exp\{i[\bar{\omega} - (\Lambda_+ + \Lambda_-)/2]t_1\}\sin[\pi J_{AB} t_1]$$

in the final density operator. This term will produce correlation peaks at $[\omega_1, \omega_2] = [\bar{\omega} - (\Lambda_+ + \Lambda_-)/2 \pm \pi J_{AB}, \omega_x]$. It may be concluded therefore that the "unexpected" correlation peaks arise from proton–proton magnetization transfer via strong coupling during the evolution period.

*(e) 2D DQ INADEQUATE experiment.* One of the most powerful NMR assignment techniques available for large organic molecules is the 2D DQ INADEQUATE experiment (*18–25*) since it is capable of tracing out the molecular framework by correlating the $^{13}C$ chemical shifts of coupled (directly bonded) carbon atoms. Bax and Freeman (*26*) have considered the behavior of an AB spin system during the INADEQUATE experiment, and have used element-by-element density matrix calculations to determine the $\tau$ dependence of the total double-quantum coherence generated in the sequence

$$\pi/2(\phi_1)\text{—}\tau\text{—}\pi(\phi_2)\text{—}\tau\text{—}\pi/2(\phi_3)\text{—}t_1\text{—}3\pi/4(\phi_4)\text{—}t_2\text{—Acquire,}$$

but did not deal with the explicit intensities of the various lines within the 2D DQ

INADEQUATE spectrum. The evolution of the density operator during the INADEQUATE sequence is

$$A_0 + B_0 \xrightarrow{\pi/2(A_x + B_x)} \xrightarrow{\mathscr{H}\tau} \xrightarrow{\pi(A_x + B_x)} \xrightarrow{\mathscr{H}\tau} (2A_{+1}B_0 + 2A_0B_{+1})$$

$$\times \{(\delta\omega/\Lambda)^2 + (\pi J_{AB}/\Lambda)^2\cos(2\Lambda\tau)\}/(2\sqrt{2}) \xrightarrow{\pi/2(A_x + B_x)} \xrightarrow{\mathscr{H}t_1}$$

$$(-i/4)(2A_{+1}B_{+1})\{(\delta\omega/\Lambda)^2 + (\pi J_{AB}/\Lambda)^2\cos(2\Lambda\tau)\}\exp[-2i\bar{\omega}t_1]$$

$$\xrightarrow{(3\pi/4)(A_x + B_x)} \xrightarrow{\mathscr{H}t_2}$$

$$(A_{-1} + B_{-1})\{(1 - \pi J_{AB}/\Lambda)\sin[(\Lambda + \pi J_{AB})t_2] + (1 + \pi J_{AB}/\Lambda)\sin[(\Lambda - \pi J_{AB})t_2]$$

$$- i(A_{-1} - B_{-1})(\delta\omega/\Lambda)\cos[(\Lambda + \pi J_{AB})t_2] - \cos[(\Lambda - \pi J_{AB})t_2]\}\exp[i\bar{\omega}t_2]$$

$$\times \{[(\delta\omega/\Lambda)^2 + (\pi J_{AB}/\Lambda)^2\cos(2\Lambda\tau)]\sin(2\pi J_{AB}\tau) - (\pi J_{AB}/\Lambda)\sin(2\Lambda\tau)\cos(2\pi J_{AB}\tau)\}$$

$$\times \exp[-2i\bar{\omega}t_1]\{(1 + \sqrt{2})i/(16\sqrt{2})\}. \quad [28]$$

The term in $A_{-1} + B_{-1}$ in the final density operator is the detected signal and corresponds to peaks at $[\omega_1, \omega_2] = [2\bar{\omega}, \bar{\omega} \pm (\Lambda + \pi J_{AB})]$ with intensity proportional to $(1 - \pi J_{AB}/\Lambda)\{(\delta\omega/\Lambda)^2 + (\pi J_{AB}/\Lambda)^2\cos(\Lambda/(2J_{AB}))\}$, and peaks at $[\omega_1, \omega_2] = [2\bar{\omega}, \bar{\omega} \pm (\Lambda - \pi J_{AB})]$ with intensity proportional to $(1 + \pi J_{AB}/\Lambda)\{(\delta\omega/\Lambda)^2 + (\pi J_{AB}/\Lambda)^2\cos(\Lambda/(2J_{AB}))\}$ for $\tau = 1/(4J_{AB})$. The intensities of the lines are proportional to the double-quantum coherence intensity given by Bax and Freeman (*26*), and the relative intensities in the $\omega_2$ dimension are just those of the conventional AB spectrum. It should be noted that the "inner" lines of the AB spectrum will have significantly greater intensity than the "outer" lines, and the "inner" lines should be observable in the 2D DQ INADEQUATE spectrum under less stringent conditions than those discussed by Bax and Freeman (*26*).

## CONCLUSIONS

We have shown how the simple product basis operators for AB and ABX systems evolve during free precession. The detailed examples presented demonstrate the applicability of the results. Further, but more qualitative, applications involve the explanation of pathways by which unexpected peaks in RELAY (*27*) and other experiments on strongly coupled systems can arise. We anticipate that these qualitative descriptions will be most useful to workers in the field.

## ACKNOWLEDGMENTS

The authors gratefully acknowledge helpful discussions with Dr. T. T. Nakashima. This work was supported by the Natural Sciences and Engineering Research Council of Canada.

## REFERENCES

1. O. W. SØRENSEN, G. W. EICH, M. H. LEVITT, G. BODENHAUSEN, AND R. R. ERNST, *Prog. NMR Spectrosc.* **16,** 169 (1983).
2. K. J. PACKER AND K. M. WRIGHT, *Mol. Phys.* **50,** 797 (1983).
3. A. KUMAR, *J. Magn. Reson.* **30,** 227 (1978).

4. M. A. THOMAS AND A. KUMAR, *J. Magn. Reson.* **56,** 479 (1984).
5. T. T. NAKASHIMA AND R. E. D. MCCLUNG, *J. Magn. Reson.* **70,** 187 (1986).
6. C. P. SLICHTER, "Principles of Magnetic Resonance," 2nd ed., Springer, Berlin, 1978.
7. J. A. POPLE, W. G. SCHNEIDER, AND H. J. BERNSTEIN, "High-Resolution Nuclear Magnetic Resonance," McGraw-Hill, New York, 1959.
8. J. BRAUNSCHWEILER AND R. R. ERNST, *J. Magn. Reson.* **53,** 521 (1983).
9. G. BODENHAUSEN, H. KOGLER, AND R. R. ERNST, *J. Magn. Reson.* **58,** 370 (1984).
10. A. D. BAIN, *J. Magn. Reson.* **56,** 418 (1984).
11. A. BAX, "Two-Dimensional Nuclear Magnetic Resonance," Delft Univ. Press, Delft, 1982.
12. G. WIDMER, R. BAUMANN, K. NAGAYAMA, R. R. ERNST, AND K. WÜTHRICH, *J. Magn. Reson.* **42,** 73 (1981).
13. L. E. KAY, J. N. S. SCARSDALE, D. HARE, AND J. H. PRESTEGARD, *J. Magn. Reson.* **68,** 515 (1986).
14. S. MACURA AND R. R. ERNST, *Mol. Phys.* **41,** 95 (1980).
15. O. SØRENSEN, M. RANCE, AND R. R. ERNST, *J. Magn. Reson.* **56,** 527 (1984).
16. T. T. NAKASHIMA, B. K. JOHN, AND R. E. D. MCCLUNG, *J. Magn. Reson.* **59,** 124 (1984).
17. T. T. NAKASHIMA, private communication.
18. A. BAX, R. FREEMAN, AND T. A. FRENKIEL, *J. Am. Chem. Soc.* **103,** 2102 (1981).
19. A. BAX, R. FREEMAN, T. A. FRENKIEL, AND M. H. LEVITT, *J. Magn. Reson.* **43,** 478 (1981).
20. T. H. MARECI AND R. FREEMAN, *J. Magn. Reson.* **48,** 158 (1982).
21. N. S. BACCA, M. F. BOLANDRIN, A. D. KINGHORN, T. A. FRENKIEL, R. FREEMAN, AND G. A. MORRIS, *J. Am. Chem. Soc.* **105,** 2538 (1983).
22. D. L. TURNER, *J. Magn. Reson.* **53,** 259 (1983).
23. C. J. TURNER, *Prog. NMR Spectrosc.* **16,** 311 (1984).
24. D. L. TURNER, *Prog. NMR Spectrosc.* **17,** 281 (1985).
25. G. A. MORRIS, *Magn. Reson. Chem.* **24,** 371 (1986).
26. A. BAX AND R. FREEMAN, *J. Magn. Reson.* **41,** 507 (1980).
27. L. E. KAY, P. J. JONES, AND J. H. PRESTEGARD, *J. Magn. Reson.* **72,** 392 (1987).